



Towards Automation of Aerial Refuelling Manoeuvres with the Probe-and-Drogue System: Modelling and Simulation

Nicolas Fezans
DLR (German Aerospace Center)
Research Scientist
DLR-FT-FDS, Lilienthalplatz 7, 38108 Braunschweig
nicolas.fezans@dlr.de

Thomas Jann
DLR (German Aerospace Center)
Research Scientist
thomas.jann@dlr.de

ABSTRACT

DLR is presently investigating the use of automation techniques to support pilots during aerial refuelling manoeuvres with the so-called probe-and-drogue system. During aerial refuelling manoeuvres the tanker and receiver aircraft need to fly very close to each other and this close proximity induces a very significant aerodynamic interaction between them. In order to develop new assistance / automation function for aerial refuelling and to test them in piloted simulations, real-time simulation models including all the relevant effects must be developed. Unlike in many other works with similar modelling needs, Reynolds-Averaged Navier Stokes (RANS) CFD computations were preferred to more simple techniques for the modelling of the aerodynamic interaction between tanker, receiver, hose, and drogue. The real-time simulation environment developed contains two complete aircraft models, which can both be controlled by the pilots either manually or through the auto flight functions. With other words, the tanker is no point mass model with prescribed trajectory, but dynamically reacts to external disturbances and the external disturbances affect both aircraft in a representative way. The dedicated aerial refuelling systems are also modelled and the whole infrastructure was ported to the DLR AVES simulator, such that complete refuelling manoeuvres can be flown by the pilots in a realistic environment, in order for the pilots to assess novel automation/assistance functions. This paper gives both a general overview on the modelling work performed and some specifics on selected parts of the model and the developed simulation infrastructure.

KEYWORDS: AAR, aerial refuelling, formation flight, flight control, probe-and-drogue

1 AIR-TO-AIR REFUELLING

Air-to-air or aerial refuelling (AAR) is a challenging manoeuvre of strong strategic relevance in present military operations and air power concepts. AAR consists in transferring fuel from one aircraft to another during flight. The transferred fuel is generally meant to be used by the receiver aircraft during the same flight with the aim to remain airborne longer (thereby extending its range and endurance). Many military missions as organized and flown nowadays do require one or several in-flight refuelling(s).

There are two main air-to-air refuelling technologies currently in use: the so-called probe-and-drogue and boom-and-receptacle technologies [1]. The probe-and-drogue system (see Fig. 1a) consists of a hose (which can be deployed and retracted in flight) equipped with a cone-shaped refuelling basket. The pilot of the receiver aircraft manoeuvres the receiver such that the probe is inserted into this refuelling basket. This permits to connect both fuel systems and allows the transfer of fuel from the tanker to the receiver. In the probe-and-drogue system, the main part of the refuelling system on the tanker's side is usually contained in a pod mounted under the wing. The hose can be deployed through an opening on the aft of the pod (case shown in Fig. 1a). In the A400M, the refuelling

system can also be mounted at the aft of the cargo compartment and the hose can be deployed through an opening in the cargo door (door remains closed).

The boom-and-receptacle – also called flying boom – system consists of an articulated tube located under the rear of the tanker aircraft fuselage. It can be deployed and controlled by a dedicated operator by means of two movable aerofoils that act as control surfaces as it can be seen in Fig. 1b. The pilot of the receiver aircraft does not actively establish the contact with the boom, but need to position the receiver within a small volume located under the tail of the tanker and to follow the instructions of the boom operator. A receptacle for the boom is located on the upper side of the receiver aircraft. Once the receiver aircraft is in position, the boom operator drives the boom into that receptacle and establishes the contact. In most tanker aircraft, the boom operator station is placed in direct-sight of the boom and receiver aircraft. In recent tankers (e.g. Airbus A330 MRTT and Boeing KC767) the boom operator stations are not located at the rear of the aircraft anymore. The boom operator can still observe the receiver and the boom via video cameras, while benefiting of more comfortable operator station.



a) Probe-and-drogue system. Author: SSgt. Suzanne M. Jenkins, U.S. Air Force.

b) Boom-and-receptacle system during the refuelling of an F-16 by a KC135 seen from the boom operator station. Author: MSgt John E. Lasky, U.S. Air Force.

Figure 1: View of the two main air-to-air refuelling technologies currently used: probe-and-drogue and boom-and-receptacle. Pictures U.S. Air Force, in the public domain.

The work presented in this paper is part of a broader activity at DLR in which the potential of new automation functions and technologies for air-to-air refuelling tasks is investigated. Even if aerial refuelling has been used for decades, this remains a very difficult piloting task for which almost no assistance is provided to the pilot in spite of all the possibilities of modern flight control systems. The aim of the whole program is therefore to investigate novel pilot assistance systems for aerial refuelling and also to investigate the possible system concepts enabling a fully automatized aerial refuelling. The latter is especially interesting for UAV receivers for which the delays in the datalink is making it very difficult (if not impossible) to perform such a high-gain piloting task remotely. In order to be able to develop and assess the various assistance concepts that will be investigated in this on-going research activity, good simulation models are required. Such a model shall include realistic aircraft models (both tanker and receiver) as well as the various components of the AAR system itself. Additionally, representative refuelling scenarios have to be defined and the simulation infrastructure must be able to fit all the needs of these scenarios. This paper presents an overview on the on-going AAR modelling and simulation activities performed at DLR with the aim of enabling future research on AAR pilot assistance systems.

The work currently performed at DLR on air-to-air refuelling focuses on the probe-and-drogue refuelling system. An argument against the probe-and-drogue system and for the boom-and-receptacle system was that the majority of the tanker fleet of the NATO nations belongs to the USA. Another argument is that the maximum fuel rate is higher with the boom-and-receptacle system. However, the fact that the German Air Force and many other NATO partners, European partners, and many other NATO “partner for peace” countries use almost exclusively this system (and will probably continue to use this system in the years/decades to come) motivates to focus on the probe-and-drogue system in the present work. Even if the portfolio of European tankers include tankers

equipped with the boom-and-receptacle system (e.g. the different variants of the A330-MRTT and A310-MRTT), these aircraft can be (and usually are) equipped with the probe-and-drogue system. Finally, the A400M which is currently entering into service is expected to represent soon the majority of the European tanker-capable aircraft fleet. The A400M can (at least until now) only be equipped with the probe-and-drogue system. As it can be seen in Fig. 2, the A400M can also be equipped with a probe and be refuelled with this system.

This paper consists of two main parts. Section 2 focuses on the considered scenarios and the flight physics modelling. Section 0 presents an overview of the way this model is implemented as well as some selected aspects for which further details are provided.



Figure 2: Side and front views of the probe on the A400M. Pictures taken on May 22nd 2014 during the ILA Air Show in Berlin, Germany. Copyright N. Fezans.

2 SCENARIO AND MODELLING

2.1 Considered Scenario

In terms of aircraft pairing, there are mainly two kinds of operationally relevant refuelling scenarios: a large tanker aircraft refuelling a significantly lighter aircraft (often a fighter) and a large tanker aircraft refuelling another large and heavy airplane (possibly even larger than the tanker). In terms of automation the latter case appears to be more challenging, due to the fact that the large receiver aircraft are usually less agile than the lighter receiver aircraft. Consequently, the considered scenario involves a large tanker aircraft and a large receiver aircraft. Previous work made at DLR led to define the so-called "Future Military Transport Aircraft" (FMTA) as an A400M-like configuration with sufficient differences from the original A400M to benefit from a certain amount of freedom for research and publications. Quite detailed dynamic models of FMTA have been developed during previous projects [2,3,4,5,6]. Besides, a scenario with an A400M refuelling another A400M is meaningful from an operational point-of-view. Consequently, only the air-to-air refuelling of an FMTA with another FMTA is considered in the manned-aircraft part of this work.

This work is part of a research project in which the refuelling of unmanned aircraft is also addressed; however this paper focuses on the manned receiver case. The flight point chosen for this scenario corresponds to a typical refuelling flight point for both large aircraft and fighter aircraft (both as receivers): FL200 with $V_{CAS} = 260$ kts.

2.2 Operational Procedure

There are plenty of standardized air-to-air refuelling procedures [7] within the NATO alliance and among all these procedures the so-called RendezVous Alpha (RVA α) is one of the most commonly used. As a consequence, the RVA α procedure has been selected for the present work. The RendezVous Alpha procedure takes place along a predefined holding pattern that is specified by an anchor point, a leg orientation (χ_{Leg}), a leg length, and the distance between the legs (see Fig. 3). The used procedure is expected to have no or only very little influence on the evaluations made of the various assistance/automation functions developed during this work, such that – at the current stage of the investigations – it does not appear useful to consider more than one procedure.

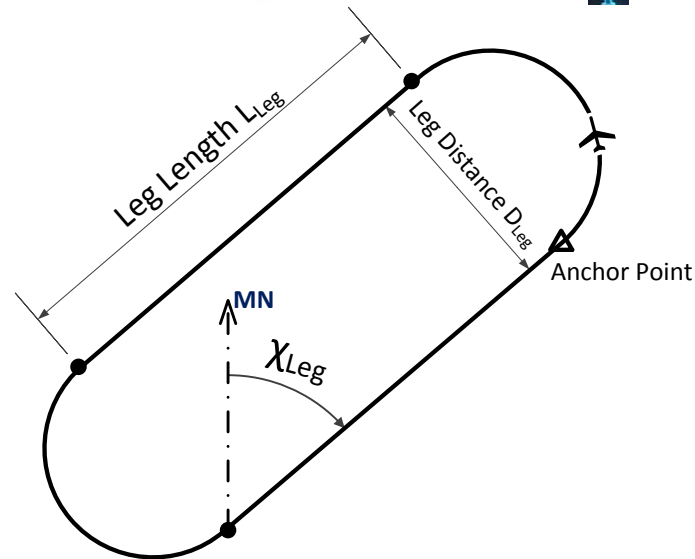


Figure 3: Race-track holding pattern followed by the tanker and the receiver.

2.3 Tanker and Receiver Flight Dynamics and Their Aerodynamic Interaction

2.3.1 Origin of the Interaction and Use of Computational Fluid Dynamics to Produce the Required Data

When flying far from each other, both aircraft can be seen as separated models with no interaction whatsoever. When both aircraft begin to fly relatively close to each other but still with no significant aerodynamic interaction (e.g. slightly different altitudes or lateral positions) some coupling must be introduced between both models. In this case, their dynamics stay uncoupled but the external conditions encountered by each aircraft (weather, temperatures, turbulence, etc.) are now partly correlated and this correlation must be modelled.

Finally, when one of the aircraft (usually the receiver) approaches or flies into areas in which the wind field velocities induced by the other aircraft (usually the tanker) are large enough to induce a significant change of the aerodynamic forces and moments, these effects must be modelled. Most of the aerodynamic interaction between both aircraft during aerial refuelling occurs at distances (along the flight path) lower than a few wingspans of the leading/tanker aircraft. In this type of situations, approximations of the induced flow field using the various well-known wake-vortex models reach their limits because the roll-up process is not achieved at such short distances and secondary effects (e.g. due to the engine blow/propellers and due to the fuselage) cannot be fully neglected. The approach shown in [8] shall be able to tackle the vortex roll-up issue and constitute a good compromise between complexity and precision but still lacks the modelling of the secondary effects.

Due to the need for a wide ramp door, the aft of the fuselage of a military transport aircraft is generally less aerodynamically efficient than those of a typical airliner and the corresponding effects are not very easy to compute with simplified approaches. For the proper computation of the flow field in the case of the air-to-air refuelling with a probe-and-drogue system at the aft of the cargo compartment (i.e. not attached to a pod under the wing) and whose hose passes through the ramp door, RANS CFD seems to be the most appropriate technique. Panel methods might provide interesting results, but in the absence of adequate validation data, RANS CFD was preferred. A series of steady RANS CFD computations were performed with the DLR TAU flow solver [9,10,11,12] to compute the complete wind field around and behind the tanker. In order to prevent the dissipation of the wake in the computed solution, the mesh was specially refined in the interesting areas, as shown in Fig. 4. A large box of roughly 4 fuselage lengths * 2 semispans * 2.3 semispans was refined in the mesh (half model computations). Additionally, the domain around the aircraft nose was also refined in order to compute precisely the so-called bow wave effect. The bow wave describes the disturbed flow field around the nose of the receiver aircraft close to the probe, which tends to push the drogue away from the aircraft nose when trying to establish contact with a probe located near to the aircraft nose/bow [13,14,15,16,17,18].

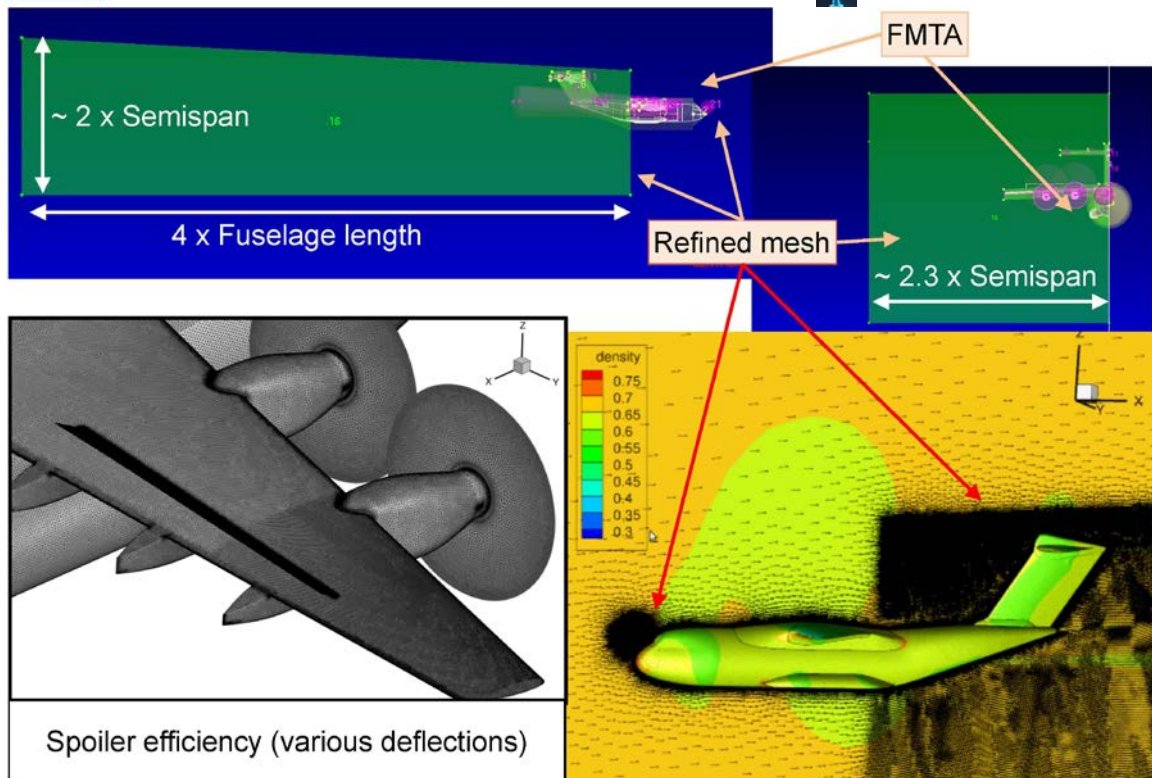


Figure 4: Overview of the CFD Computations Supporting the Modelling Activities.

The DLR TAU flow solver is developed by the DLR Institute of Aerodynamics and Flow Technology [9,10,11,12]. It solves the compressible 3D RANS equations, using a finite volume formulation. For these simulations a cell vertex metric is used with a multigrid approach. Moreover a hybrid grid with a total amount of $50 \cdot 10^6$ nodes with 36 prismatic layers to resolve the boundary layer close to the wall and a tetrahedral grid to resolve the outer flow field are used. With a grid refinement of the prismatic layers close to the wall, a dimensionless wall distance of $y^+ < 2$ could be achieved. Additionally the one equation Spalart-Allmaras turbulent model [19] in its negative form is applied.

During the entire aerial refuelling manoeuvre the relative positions, orientations as well as the relative motion between the two airplanes vary very much such that computing all possible cases or even at least a significant number of the possible situations would be extremely expensive and time-consuming. At some point in the future, probably in about two decades from now, the computational power available will permit to tackle this kind of modelling and simulation (including dynamic motion) of the two aircraft in close proximity with unsteady RANS CFD techniques. The approach chosen here consists in computing with RANS CFD techniques the flow around the tanker, alone, for the different relevant conditions (mass or lift variations are required, but possibly also variations of thrust and of the flight points). The complex wake in close proximity of the tanker is then extracted and used as input for low-level aerodynamics methods (see section 2.3.2 and references [20,21,22]) allowing the computation (in real-time) the additional forces and moments generated by the inhomogeneity of this wake on the receiver airframe.

As a consequence, the boundary conditions used in the RANS CFD calculations of the tanker alone are quite standard boundary conditions: the far-field boundary conditions are set to the airspeed vector for the relevant values of the angle of attack and angle of sideslip. Additionally a symmetry plane is used to reduce the grid size from a full model to a half model. Finally the propellers are modelled as actuator disks with an inlet and outlet panel. An aerodynamic dataset together with the speed and the pitch angle of the blades describe the changes of the flow within the actuator disk. With it the unsteady aerodynamic due to the propeller can be simulated as a quasi-steady-state model.

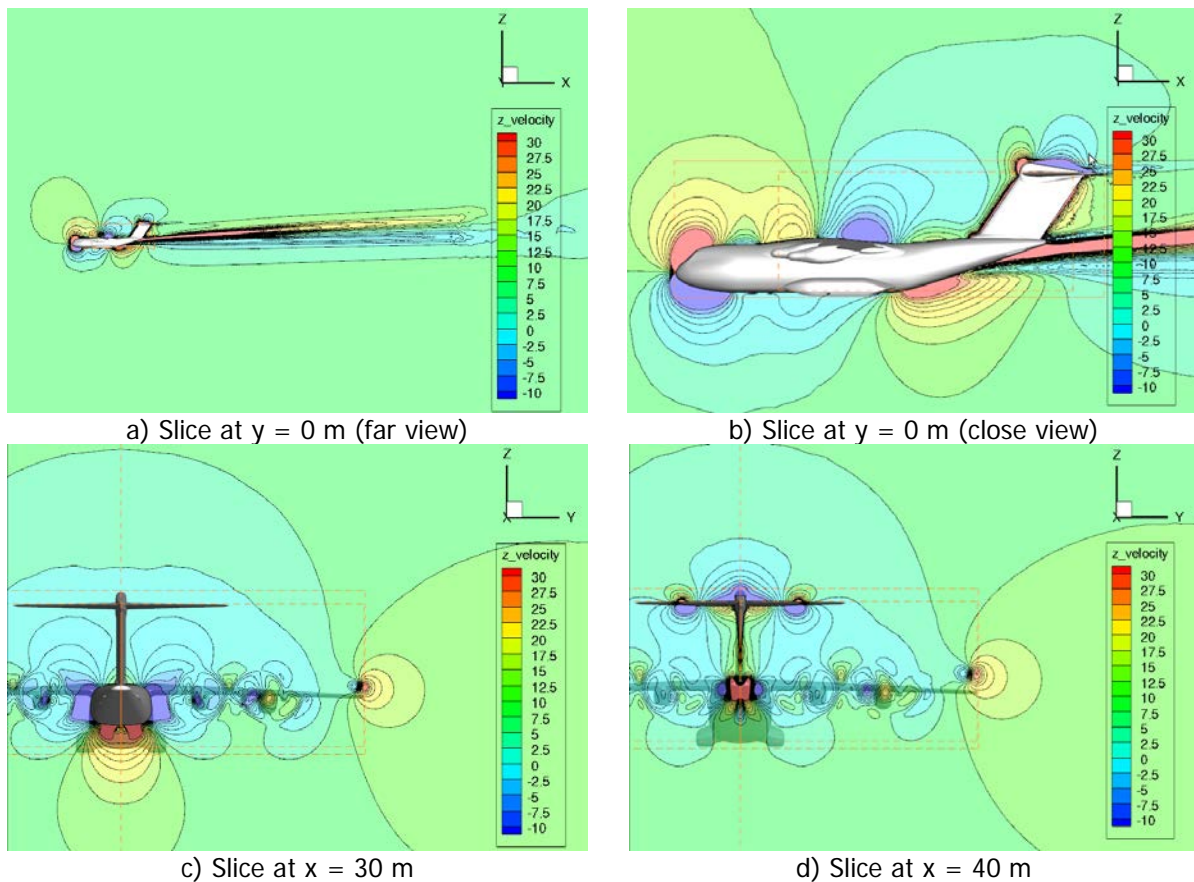


Figure 5: Illustration of the Typical Flow Characteristics That Can Be Found in the Wind Fields Computed with RANS-CFD. $V_{CAS} = 260$ kts, $H = 20,000$ ft.

Various slices across one of the CFD solutions are shown in Fig. 5. Note that in this figure, the coordinates are body-fixed, with the origin roughly at the aircraft nose, and the signs as typically defined in aerodynamics (x pointing backward, y to the right, and z upward). Consequently, a z -velocity that is higher than the average, far-field z -velocity corresponds to an induced upwash, whereas a z -velocity that is lower than the average, far-field z -velocity corresponds to an induced downwash. For instance, the bow-wave effect [13,14,15,16,17,18] can be seen in Figs. 5a and 5b by the induced downwash (i.e. cyan/blue) under the aircraft nose and the induced upwash (i.e. yellow/orange/red) above it. In these figures, it can also be observed that directly behind the ramp door, a significant upwash is induced, even if the wake vortices eventually (i.e. further behind the aircraft) are dominating (downwash). The receiver aircraft wings will be located in this downwash during the refuelling, but quite different flow conditions are encountered along the refuelling hose. Figs 5c-5d also show the vertical velocity in two separate planes at the tail of the aircraft. The beginning of the vortex roll-up can be observed through the upward induced wind right from the right wing tip and the slight downwash behind the wings. The latter is more difficult to observe due to the propeller swirls and due to the effects of the high-lift fairings and of the engine nacelles.

The high-quality CFD results are a great support for the modelling of the flow induced by the tanker aircraft and around the nose of the receiver aircraft. After having imported the TAU solutions into the software packet TecPlot 360, the wind velocities in the CFD results are exported for all points of some rectangular grids.

These data will be imported in the real time simulation model and currently various grids and resolutions are still being tested. The amount of data is such that a compromise must be made between the precision and the memory usage to load all these data. At this stage of the investigations it seems quite likely that the final implementation will use representation with a location-dependent resolution: A higher resolution will probably be used around particular flow field



features (e.g. the wake vortex cores), whereas a lower resolution will probably be used in areas where the induced wind is relatively homogeneous.

2.3.2 Modelling the Impact of Inhomogeneous Flow Onto the Receiver, the Hose, and the Drogue

Once the inhomogeneous flow field induced by the tanker had been determined, its impact onto the aerodynamic forces and moments for the receiver need to be modelled. This corresponds exactly to what is known in the wake-vortex community as “Aerodynamic Interaction Model” (AIM). A good overview of the different approaches for generating an AIM can be found in [20] (section IV) and the references therein. The strip method from [21,22] is adapted to the FMTA geometry and used in the current work.

2.3.3 Improved Spoiler Effectiveness Model

As suggested by the lower-left part of Fig. 4, CFD computations were also used to improve the FMTA model regarding the spoiler aerodynamic efficiencies. This was required because some of the flight control concepts that will be investigated for the aerial refuelling phase involve the use of the spoilers as a mean for direct lift control (DLC). This allows the receiver to partly control the lift independently from the angle of attack. A symmetrical deflection of the spoilers (similar but not necessarily equal in behaviour to the speedbrake function) reduces the lift generated on the wing: by commanding a permanent deflection of the spoilers and by dynamically increasing or decreasing this deflection the lift can be respectively decreased or increased. Symmetrical spoiler deflections have also other effects on drag and on the pitching moment, which can be both compensated such that a pure direct lift control can be realized in practice.

2.4 **Probe-and-Drogue Modelling**

The selected scenario presently considers the centreline hose and drogue refuelling (Fig. 6), but can also be adapted to refuelling systems using PODs. The flexible hose is controlled by the so-called hose drum unit (HDU), which is located inside the FMTA tanker aircraft directly behind the closed ramp door. When fully deployed the hose has a trailing length of 24 m (\approx 80 ft), while a diameter of 0.068 m (2.6 inch) and a specific “wet” weight of 4 kg/m were assumed according to [23]. The high speed drogue is modelled with a drag area of 0.186 m² (2 ft²) and a weight of 30 kg (65 lbs).

Two modelling approaches are used: a physically deduced multi-body model and a simpler replacement model, which are implemented as a subsystem in the overall model including tanker and receiver aircraft. The first approach is a lumped mass model with 50 coupled point masses. In Fig. 7 the masses are located in the joints 1 to 50 connected by rigid or semi-rigid (elasticity only in longitudinal direction) and mass-less segments. Each of these point masses has a drag coefficient associated with it and reacts accordingly to the local airflow at its position. For reeling the hose out or in, only the closest segment to the HDU is modified between zero and maximum length, until the next joint appears or disappears at the fairing. The drogue is modelled as rigid body, having a conical geometry and adequate aerodynamics creating also side and lift forces. This is important in order to respond realistically to the bow wave. A contact model takes into account the conical inner and outer geometry of the drogue creating the proper reaction in case of collision between the probe and the inner or outer drogue surfaces. This approach is quite similar to the modelling made in [23,24,25,26,27] for the whole assembly. [15,28] contain interesting data for the aerodynamic modelling of the drogue. A higher-order modelling approach of the hose – based on flexible elements – was proposed in [29]: this approach shall permit to reduce the number of elements, compared to a model based on rigid or semi-rigid elements. However, the equations are significantly more complicated when using flexible elements and therefore this approach was not selected for the present work.

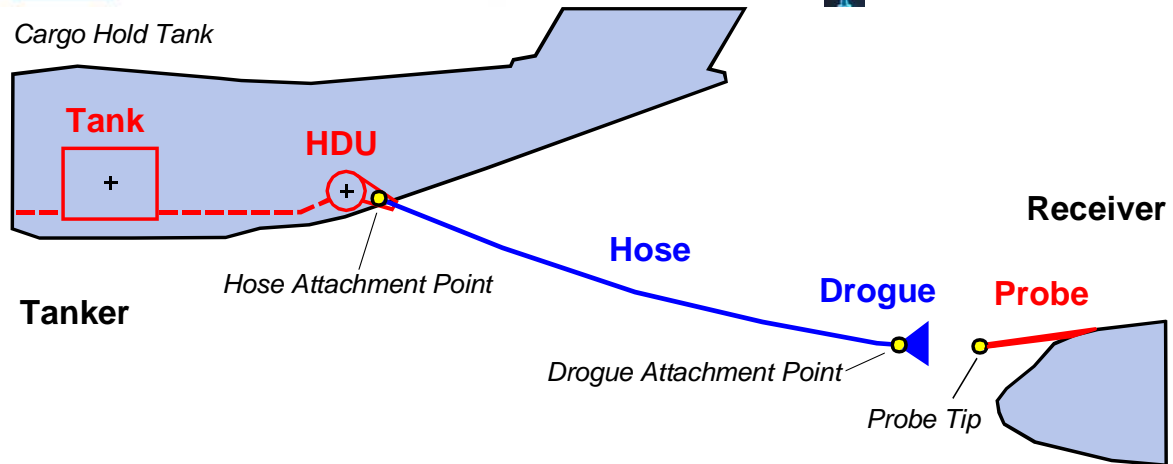


Figure 6: Sketch of the aerial refuelling configuration with the probe-and-drogue system.

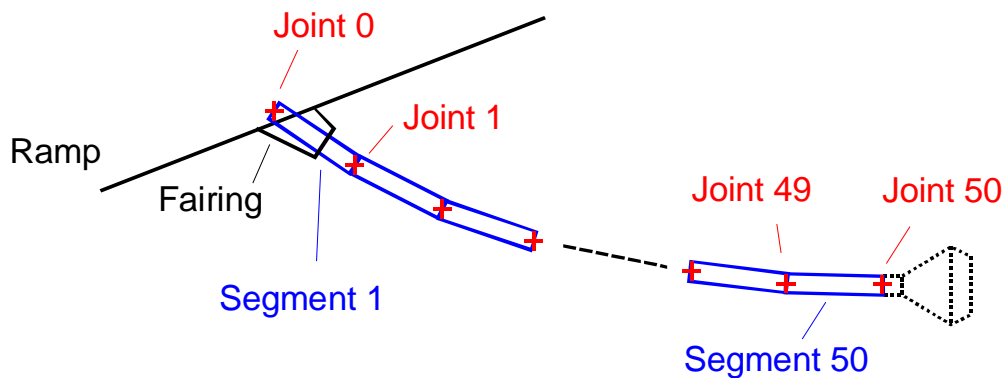


Figure 7: Geometrical representation of hose model using 50 rigid segments connected by 51 joints.

The multi-body model of the hose and drogue allows studying dynamic effects of the hose and drogue system like hose whip [25,26,27,30], whereas the simple model approximates the behaviour only in a very simplified manner. In the simple model, the drogue is modelled as a point mass reducing the aerodynamic forces to drag only. The hose is modelled as a mass-less line with a viscoelastic characteristic. The shape of the trailing hose is approximated by a parabola providing also the coordinates of the single joints for the subsequent visualization as illustrated in Fig. 7. In this simplified model the contact between the probe and the drogue is modelled with a unidirectional magnet-like attractor, which lets the drogue being caught by the probe tip when coming close enough.

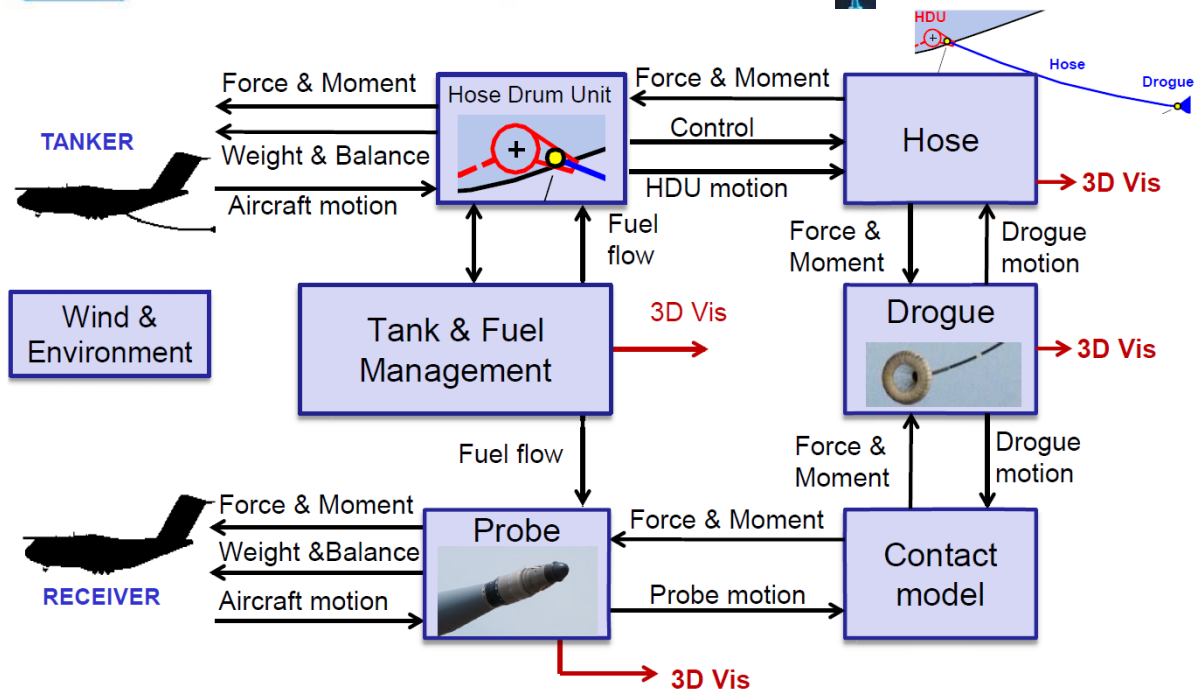


Figure 8: Overview of the probe-and-drogue refuelling model internal structure (“3D Vis” = link to the 3D visualization program).

Fig. 8 shows the modules of the refuelling subsystem. The block structure is equal for both the simple and the multi-body hose/drogue models. The external interfaces of both models are identical, such that they can be exchanged easily in the simulation programs. The refuelling control signals are connected to the so-called tanker control station, a virtual tanker cockpit, providing (among others) the hose reel in/out command, preset fuel quantities, commanded fuel flows, as well as corresponding indicators for offloaded fuel, signal light status, and many others on an emulated AAR panel.

For readability reasons in Fig. 8, a block called “Wind & Environment” is placed aside of all other blocks (and with no connection to them) to symbolize that the wind field surrounding both aircraft as well as other physical properties – such as gravity and atmospheric quantities – are impacting/interacting with all parts of the model.

2.5 Refuelling Systems Modelling

To ensure compatibility among the different tanker and receiver aircraft used by NATO nations, the typical air-to-air refuelling equipment and procedures are standardized (see section 2.2) and described in corresponding documents [7]. For modelling the refuelling system here, the refuelling process is subdivided into 10 phases numbered from 0 to 9:

0. drogue inside pod or HDU
1. drogue reeling out
2. full trail, clear contact
3. contact, but not in refuelling zone
4. in refuelling zone, fuel flow
5. in stand-off zone, fuel flow
6. in cut-off zone
7. refuelling finished, disconnect
8. separated
9. drogue reeling in

Phases 0, 1, and 9 are active before and after the actual refuelling process. The refuelling process starts with phase 2 when the receiver actively enters the so-called refuelling box. This is the safe and permitted area behind the tanker where probe-drogue contact and refuelling shall occur. The transitions between the phases are controlled by the hose retraction status, the contact status, and the (true) fuel flow to the receiver. The refuelling status is indicated to the receiver pilot using red,



amber and green signal lights near the opening through which the hose is deployed (see later in Fig. 11a). Phase 2 and 3 are indicated by a steady amber signal light.

To enable fuel flow, the receiver has to push the drogue until the hose is retracted by the HDU and reaches the refuelling zone, which is indicated by markings on the hose. The hose retraction is accomplished by controlling the tension in the hose. In the model this controller is located together with the actuator model in the HDU block. Within the refuelling zone (phase 4) the fuel valve is opened and the transfer of fuel is indicated by a steady green light. If the drogue is pushed in too far, the hose leaves the refuelling zone and enters the stand-off zone (phase 5). In this phase fuel is still transferred, but an additional flashing amber light indicates the receiver pilot to fall back towards the refuelling zone again. Beyond the refuelling and stand-off zones the green light disappears, the amber light remains flashing, and the fuel flow is cut off (phase 3 and phase 6). When the refuelling for one receiver is finished (phase 7), a flashing green light informs the receiver pilot to disconnect (phase 8) and leave the refuelling box, allowing the next receiver - if applicable - to be refuelled. All in all the phases presented before are quite similar to the phases used in [31,32], which is not very surprising since a very detailed NATO standard [7] has been used and kept up-to-date for a very long time.

The “tank and refuelling management” block of the diagram of Fig. 8 is further detailed in Fig. 9. The core of the “tank and refuelling management” is a state machine that is located in the block called “refuelling phases and lights logic.” The three other blocks shown in Fig. 9 (“preset/reset logic,” “tank and refuelling logic,” “tank weight and balance”) are responsible for managing the fuel transfer from tanker to the receiver and its implications.

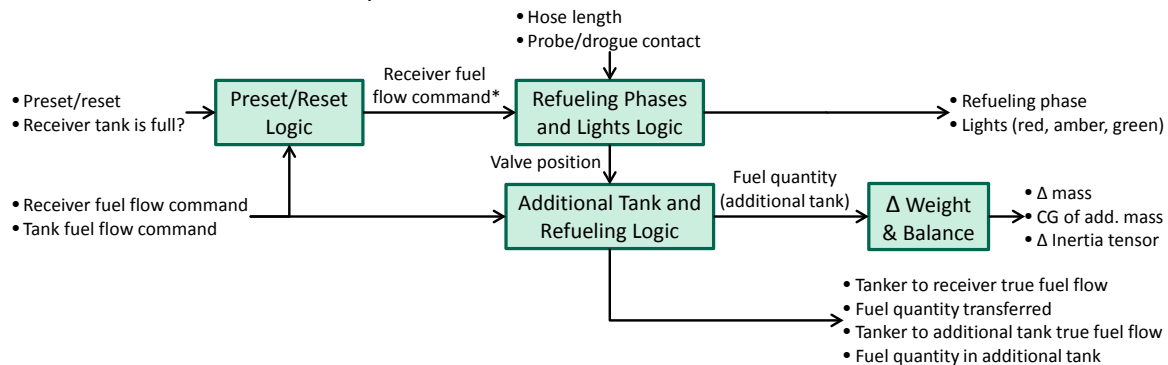


Figure 9: Internal structure of the “Tank and Refuelling Management” subsystem (Fig. 8).

The first block allows using a preset value for fuel quantity that shall be transferred. When this value is reached, the refuelling system automatically stops the fuel transfer and signals “disconnect” to the receiver. The preset value is set in the AAR panel of the tanker, where also a reset can be commanded in order to refuel the next receiver. The second block named “refuelling phases and lights logic,” as explained earlier, is responsible for stepping through the phases, setting the light signals accordingly and opening or closing the valve for fuel transfer. However, fuel can only be transferred if enough fuel is available in the tanker and the receiver tank is not full. These conditions are checked and handled in the “tank and refuelling logic” block.

In real AAR scenarios, fuel can be transferred either from additional cargo hold tanks or directly from the own fuel compartments in the tanker. In the model, a cargo hold tank is always present and working as buffer between the tanker and receiver tanks (see Fig. 6). Accordingly not only the fuel flow to the receiver, but also the fuel flow to the cargo hold tank has to be considered and controlled. Depending on the fuel level in the cargo hold tank the fuel flows to and from these tank are limited and cut off, if one of the limits is reached. Mass, inertia and CG location of the additional cargo hold tank are finally computed in the block “Tank Weight and Balance” and provided to the overall weight and balance subsystem of the tanker model. Note that the mass of fuel in the regular tanks is directly handled (in terms of weight and balance) by the basis FMTA models (tanker and receiver). However, the additional masses related to the Hose-Drum Unit, possible wing pods, additional tanks (and their content) and the probe (as it can be unmounted) are computed in the AAR subsystem and transmitted to the FMTA models such that they are properly taken into account in the equations of motion.

2.6 Correlation of Atmospheric Disturbances Encountered by Both Aircraft

In all the previous sections, elements that are specific to the aircraft, the air-to-air refuelling systems, and the wake of the tanker aircraft were presented. All these elements play a role during refuelling in all weather conditions, including in calm air. For the design of novel control functions, regardless of for full automation or for pilot assistance, the impact of external disturbances must be considered and the capability of the system to deal with them must be demonstrated, at least to some extent.

When both aircraft are flying very close to each other the atmospheric disturbances encountered by the two aircraft will be strongly correlated and this should be modelled. In the case where a space-dependent turbulence field is considered, using the local wind field for each aircraft is straightforward and leads to the adequate correlation. If a time-based turbulence generation is used (e.g. white noise through dynamic filters with Dryden or von Karman spectrums) the coupling of the turbulence between both aircraft is less direct.

In that case, the approach chosen here is to generate the turbulence for a virtual point, which is by definition always "ahead of both aircraft". This point is generated by a sequence of operations. First, the formation middle point M is defined as the middle of the segment joining the tanker T and the receiver R . The middle point velocity vector $\vec{V}_{K,M}$ is defined as the average of the tanker velocity vector $\vec{V}_{K,T}$ and the receiver velocity vector $\vec{V}_{K,R}$. The middle point M and its velocity vector $\vec{V}_{K,M}$ define a line in space. Two points of this line are particularly interesting: the projection R_M of R and the projection T_M of T on the line. The virtual point P_{ref} used for turbulence generation is then defined as the point of the aforementioned line which is located at a chosen offset ahead of the foremost point R_M or T_M based on the direction defined by the vector $\vec{V}_{K,M}$. The offset chosen does not need to be very large but just ensures that the time required for each aircraft to pass the current location of P_{ref} (i.e. being at this point or abeam of it) is positive. An offset of 10 metres is used here. Finally, the turbulence generated for point P_{ref} is a time signal that is delayed respectively of $\tau_T = T_M P_{ref} / (\vec{V}_{K,T} \cdot \vec{u}_{K,M})$ and $\tau_R = R_M P_{ref} / (\vec{V}_{K,R} \cdot \vec{u}_{K,M})$ for the tanker and the receiver. This whole process is represented graphically in Fig. 10.

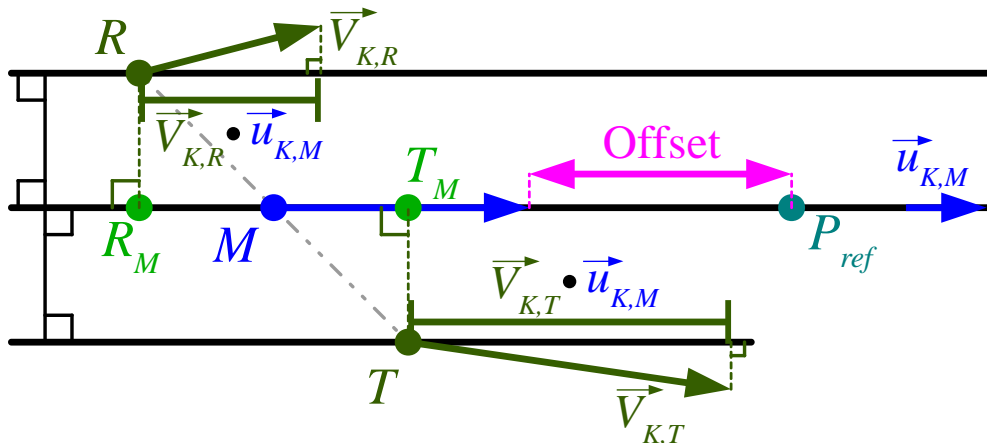


Figure 10: Representation of the turbulence correlation between the two aircraft.

In the typical aerial refuelling configuration, the receiver is flying right behind the tanker and the obtained time-delays are such that a gust will be encountered by the receiver, just after the tanker did encounter it. Even with the same aircraft type, if their mass is very different or if the flight control system is in a different mode, the reaction of the aircraft will differ. When both aircraft fly far from each other, the maximum delay could be very large and this might pose some practical issues (size of the associated buffer), as a consequence the delay was limited to 10 seconds. The whole computation shall also include any "mean wind" if present. For this, the mean wind should be added to inertial speed vectors used here, to produce "mean true airspeed vectors" which can be used as just shown.

3 INFRASTRUCTURE FOR THE SIMULATION OF AERIAL REFUELLING MANOEUVRES BETWEEN TWO FUTURE MILITARY TRANSPORT AIRCRAFT

This section presents the simulation infrastructure as well as some selected aspects related to the implementations of the dynamic model and of some of the other modules.

3.1 High-Level View of the Infrastructure

The simulation infrastructure designed for the FMTA-FMTA case is represented in the diagram of Fig. 11. The usual software architecture of the DLR AVES simulator [33,34,35] is used for the receiver aircraft and most of the software modules instantiated a second time for the tanker aircraft. The duplicated modules are identical for both aircraft, but have separated states such that both aircraft can be flown independently from each other. Note that Fig. 11 shows rather the high-level functional decomposition of the overall architecture and its main modules. The whole architecture is somewhat comparable to the architecture presented in [36,37], even though the different graphical representations used here and in these references might give the impression that the architectures are completely different. The graphical representation used in the aforementioned references is rather based on the working stations (e.g. cockpit, instructor, operator, simulation observer stations) and the physical computers.

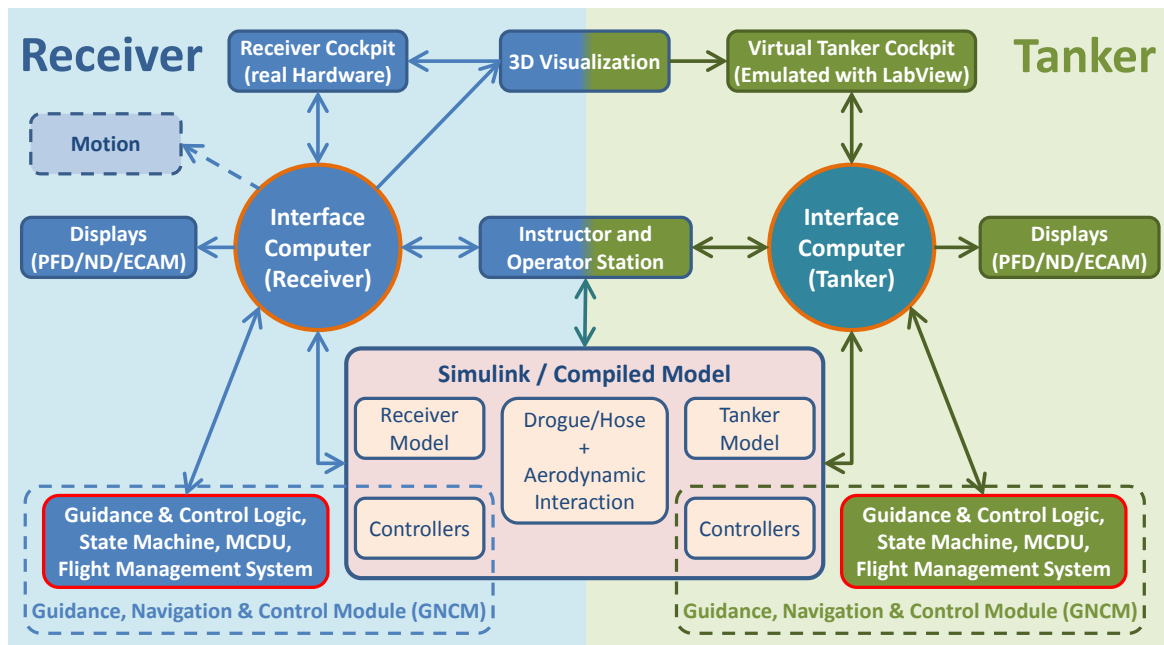


Figure 11: Overview of the different modules of the air-to-air refuelling simulation environment.

In order to easily ensure that the physical couplings between the aircraft are properly realized and simulated, both aircraft as well as all the flight physics are contained in a single Simulink model. This eliminates the need for a very tight synchronization mechanism (apart from the standard functionalities of Simulink) between the aircraft models since the right order for all computations can directly be determined by Simulink at model compile time. This also permits to avoid having to define data exchanges required for the quite complex couplings between the aircraft in an interface between two modules: these couplings remain inside the Simulink model. As a consequence, the resulting Simulink model is connected to two interface computers (IC): the one that is the central node of the “Receiver” simulation and the one that is the central node of the “Tanker” simulation. The interface definition is the same for both the Receiver-IC and the Tanker-IC connections.

In addition to having only one common Simulink model for both aircraft, two other modules are shared and not duplicated. The first one is the 3D environment and visualization program which drives (among others) the visual system of AVES (view for the receiver pilots) as shown in section 3.2. The representation of the tanker and of the probe-and-drogue in the visual system is crucial for most automation concepts that will be tested later on in the project. Even for concepts



where the complete manoeuvre would be automated, the visual impressions provided to the pilots will influence the evaluation of the system made by the pilots.

The second module that is shared by both aircraft is the so-called "Instructor and Operator Station" (IOS). The IOS is basically the module that controls the whole simulation: it permits to initialize, start, pause, and stop the simulation. It permits to modify parameters during the simulation, to trigger some faults, or just to select and observe some variables in real-time during the simulation.

Due to the fact that only one "real" cockpit is available, a "virtual cockpit" was implemented for the tanker whereas the AVES A320 cockpit is used for the receiver. Consequently, only the receiver pilots will benefit from the motion platform. The priority is given to the receiver regarding the real cockpit and the motion due to the fact that the interesting piloting task when considering the aerial refuelling using the probe-and-drogue system takes place in the cockpit of the receiver. The tanker only flies as steady as possible during the manoeuvre. Nevertheless, the tanker can turn, as for instance to follow the race-track pattern shown in Fig. 3. Even if active control of the tanker would be used in some of the considered automation concepts, then the control actions would only be taken by the flight control system and not by the tanker pilots, such that these concepts can be tested without a fully equipped tanker cockpit on a motion platform.

3.2 3D Visualization

In the AVES simulator, the 3D environment used by the visual system must integrate a realistic representation of the tanker, of the hose, of the drogue, and of the receiver probe in order for the pilots to be able to manually control the receiver airplane towards the tanker, establish contact with the drogue, and proceed to the refuelling. Such a visualization is required also when pilots shall assess the way an automatic refuelling system is behaving. The in-house 3D visualization software used in AVES has been developed since many years on the top of the OpenSceneGraph open source library and possesses – on the top of all classical 3D scene graph features – many less common features, for instance for brown-out and fog effect or realistic water visualization for maritime scenarios [38].

For the air-to-air refuelling scenario, models of the articulated hose, of the probe, of the drogue, and the hose-drum unit (including lights) were integrated in the visualization. The hose and drogue consists of 51 elements (50 hose segments + the drogue) and this regardless of the actual physical model of the hose and drogue assembly used behind the scenes. The position and orientation of each of these elements shall be determined based on the "real physical" states of the dynamical model that is simulated. This approach permits to use a very simplified physical model in some cases without having any odd visual impression provided to the pilots.

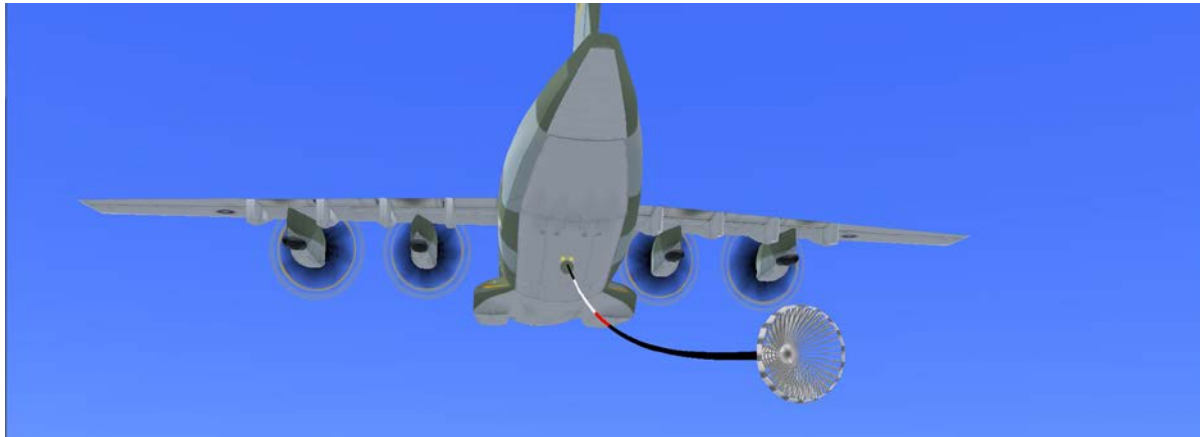
The current state of the visualization can be seen in Fig. 12. The signal lights at the HDU can be seen in Fig. 12a (two yellow dots just above the location where the hose goes through the tanker ramp door). In order to reproduce the visual impression correctly, these lights had to be made larger than they are in reality. The different lights (green, yellow, red) are located along the top side of the round HDU hose exit. The hose markings correspond to the different zones as defined in section 2.5.

3.3 Flight Control Laws and Auto Flight

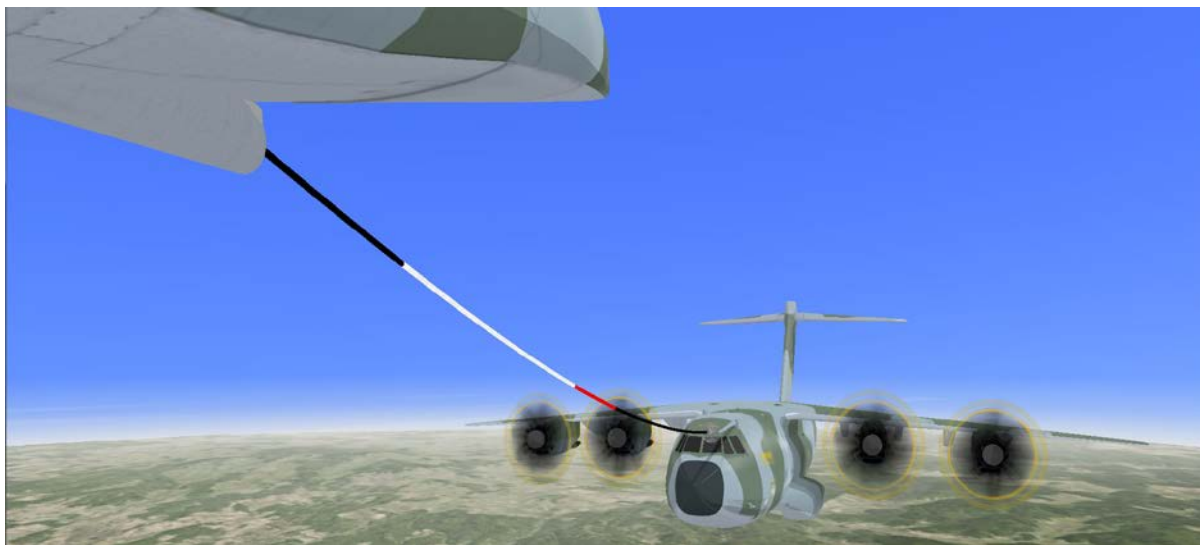
3.3.1 Overview of the Modules When Simulating the Nominal Aircraft and Regular Control Functions

The regular flight control laws (Normal / Alternate 1 / Alternate 2 / Direct) and the usual Airbus autopilot modes are implemented in the simulation environment of each aircraft. These are not the original Airbus control laws but they follow the same logic and should behave very similarly to the original ones. The various protections and limits used are currently a mix between the protections of the A400M and those of the A320 aircraft.

For each aircraft, the individual controller and autopilot modes are implemented within the Simulink model as well as the required dynamic models for the aircraft sensors. However, the complete logical conditions for the transition between the flight control modes are implemented in a separate program (one instance per aircraft) that sends the information on the currently active mode(s) to the model. The combination of both parts (in Simulink and in the separated executable) contains all Guidance Navigation and Control (GNC) functions and can be seen as one large GNC Module (GNCM).



a) View of the Tanker, HDU, and Drogue From Behind



b) View of the Receiver, its Probe, the Hose, and the Drogue

Figure 12: 3D visualization for the air-to-air refuelling simulation

The main motivation for integrating some parts of the GNCM directly with the aircraft dynamic model is that these parts are directly involved in the closed-loop dynamics: even when not simulating in an environment with strong real time guarantees (e.g. using the “AVES-on-the-Desktop” of section 0), it remains crucial to ensure that the aircraft and these parts are being simulated in a consistent and synchronous manner.

The remaining parts perform all treatments from the usual flight management and guidance computers and the flight control computers (except the pure automatic control tasks). Some of these operations (e.g. management of flight plans) are not easy to implement and to maintain using a block-diagram representation and consequently C++ code was preferred. These parts currently constitute a standalone program but could in principle also be integrated in the Simulink model as an s-function.

The quite complex state machines that manage the state of the flight controller / autopilot modes run within this program. These state machines are somewhat comparable to the ones shown in [39] but are more complex and very close to the complete original Airbus flight control/auto flight logic. This program also performs many different computations that are needed by the controllers or for the switching conditions between them (e.g. all the usual reference speeds V_{Sig} , $V_{\alpha-prot}$, $V_{\alpha-max}$, $V_{SPDFLOOR}$, the various F-speeds, etc.)



3.3.2 Definition, Integration, and Test of New Control Functions

In order to enable the development and test of new control laws/autopilot modes (one of the next steps in the current research on air-to-air refuelling automation), a possibility to integrate the new control functions in the Simulink model and activation flags/conditions must be defined. These flags are commanded by the aforementioned external program based on the current states of the different state machines. Consequently, it must be possible to define some new states for the new control functions in these state machines.

At first, the designers of the new control function need to be able to activate this new function and possibly to let pilots evaluate it in the simulator. A graphical user interface (GUI) was developed specifically for this need and permits to set the state machines in any desired mode, to reset them, or to freeze them all at once or individually (i.e. no transition is fired anymore). This permits to activate modes which are unreachable otherwise (i.e. through the transitions defined in the state machines). This GUI is meant to be used by the simulator operator and not the pilots.

Thanks to this new capability, many new modes can be defined and tested (including with pilots) without having to tackle the complexity of defining all necessary state transitions first. These transitions can however be added progressively to finally obtain a new set of flight control/auto flight logic whose entire behaviour (including transient responses and switching conditions) can be tested during representative scenarios by the pilots. This newly developed functionality will certainly be reused in many other works involving airplane simulation with Airbus-like flight control system architectures in the AVES simulator.

3.3.3 Race-Track Autopilot Mode for the Tanker

On the tanker side, a typical test in simulation of some new ideas begins with the development of a functional prototype. This functional prototype has typically a reduced functionality and is restricted to a limited set of conditions, but shall permit to make a first assessment of the idea. The functional prototype is developed and first tested on a desktop computer, in the present case using the so-called "AVES-on-the-Desktop" environment which is an almost complete virtualized version of the real AVES simulator (see [40] for further details).

As long as the idea is worth pursuing, several successive stages of development and testing are performed on the desktop, in the simulator but without type-rated pilots (i.e. typically with the engineer behind the idea and possibly some volunteers), and finally validation with professional pilots. During all these stages, most of the time tests are performed with a limited number of persons involved, sometimes even only one engineer. This can only occur if this person is able to manage the entire simulation on his/her own. For this, the regular autopilot functions of the tanker can easily be configured to fly at constant speed a straight and level trajectory. In order to fly more representative race-track trajectories as shown in Fig. 3 with no human intervention (and consequently to facilitate the testing with turn manoeuvres of the tanker) a special autopilot mode was designed. It consists of an outer-loop to classical autopilot modes (lateral: track mode, vertical: altitude hold, autothrust: speed mode) and is based on relatively simple geometrical computations.

The controller virtually tracks a point located at a so-called "look-ahead distance" (LoAh) on the desired trajectory. The reference point of the desired trajectory and from which this distance is computed is defined as the closest point of the trajectory to the current aircraft position (as the aircraft is never perfectly on the trajectory). This principle is illustrated in Fig. 13. On the configuration shown in the left part of this figure, it can be seen that if the aircraft is located on the right side of the desired trajectory the aforementioned strategy leads to follow a ground track that drives the aircraft back to the trajectory (in that case more to the left compared to the trajectory orientation). This strategy also leads to a smooth reduction of the intercept angle as the aircraft approaches the desired trajectory, as illustrated in the right part of the figure.

For the turns, the tangent of the half-circle to the closest point is taken as "reference trajectory" and the same computations as for the straight legs are performed (see Fig. 14). However, it is necessary to add an additional bank angle feedforward command to follow precisely the circle without "lagging behind". The computation of the additional feedforward bank angle command is based on the desired time derivative of the ground track angle $\dot{\chi}_{cmd}$, which itself depends on the aircraft speed and on the turn radius. Fig. 14 contains no geometrical interpretation of the feedforward term, whose equation is very known and can easily be found in textbooks on flight mechanics.

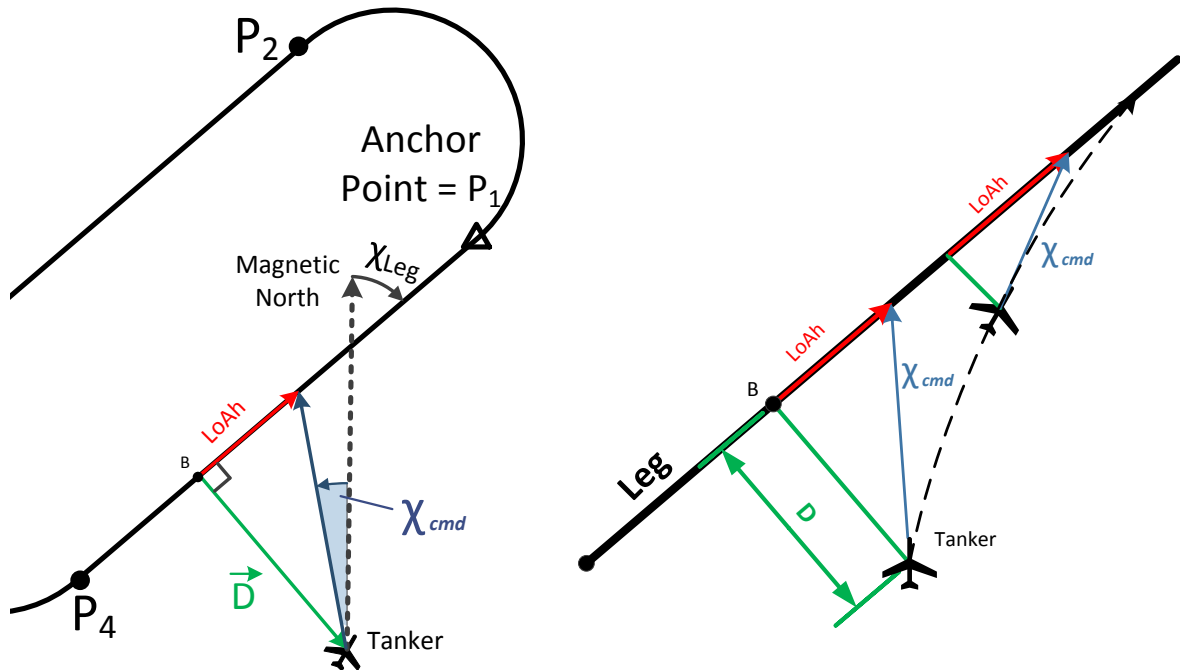


Figure 13: Race-track pattern following strategy
(left: general view, right: illustration of the resulting smooth intercept trajectory)

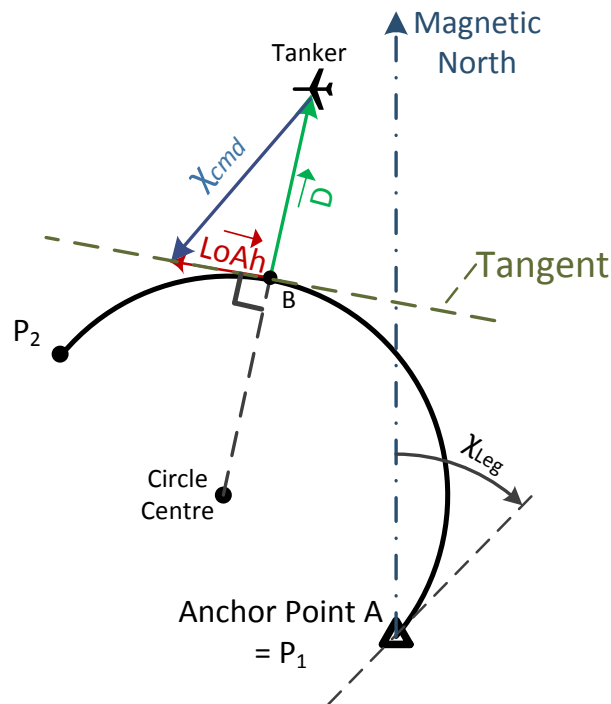


Figure 14: Same strategy based on the circle tangent during turn
(additional feedforward turn-rate-based bank angle term not represented)

A typical trajectory obtained by applying this simple strategy is shown in Fig. 15. As it can be seen in this figure, this simple strategy not only follows the track as expected but it also leads to fly a meaningful intercept trajectory when the initial location or velocity does not correspond to one of point and velocity vector of the chosen race-track. Note that there is no need for a 4D guidance scheme for this task, since the receiver pilot or control function will adapt to the real position of the tanker. The trajectory followed is based on the ground position: the wind is compensated by the controller all along the trajectory but the aircraft flies at constant airspeed (i.e. ground speed varies). Further details on the race-track controller can be found in [41].

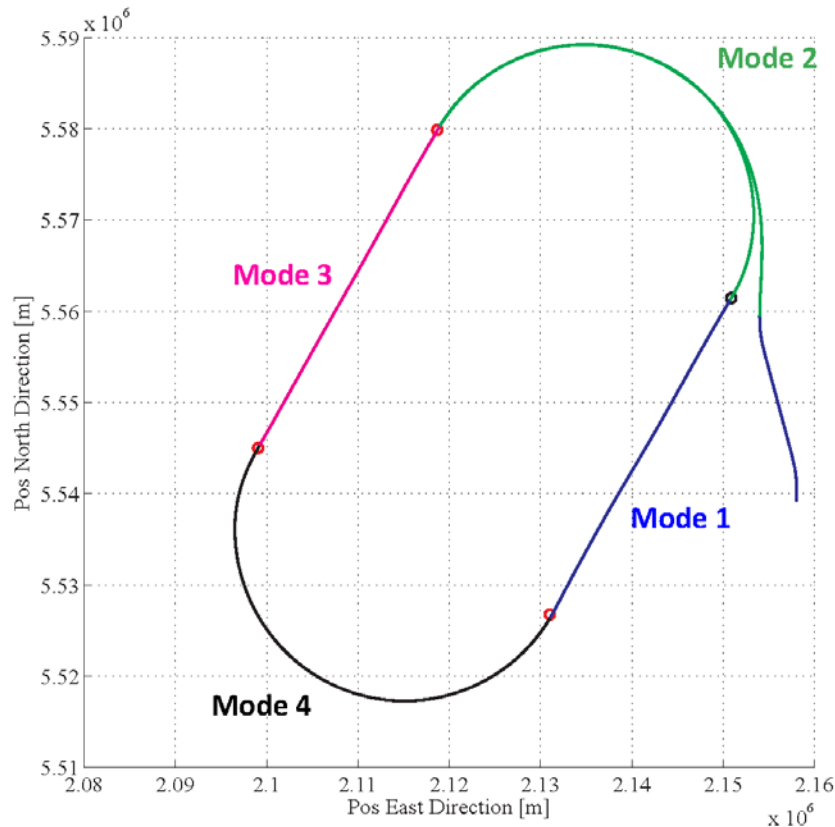


Figure 15: Illustration of the race-track pattern following behaviour

4 SUMMARY AND OUTLOOK

This paper presented an overview of the on-going modelling activities performed at DLR with the aim of supporting research on air-to-air refuelling automation for both manned and unmanned receivers. The paper mainly presented the simulation infrastructure being integrated to the existing AVES full flight research simulator. The overall infrastructure as well as some selected components were presented. For the manned receiver application a configuration with a so-called "Future Military Transport Aircraft" FMTA (an Airbus A400M-like configuration) in both tanker and receiver roles is considered. For simplicity reasons, the entire flight physics is included within one single model in this application. Other possibilities have been considered and rejected for this application, but a co-simulation principle (two separated simulation program working in a synchronous manner) has been selected for the application to the refuelling of an unmanned aircraft. This latter application is not detailed in the present paper, but the co-simulation mechanism that was developed will be published within the near future. The modelling of the interaction between both aircraft as well as the modelling of control surface nonlinearities is supported by RANS CFD computations and the a quite extensive flight control/auto flight architecture is also integrated to the simulation environment. Whilst this simulation infrastructure has been developed for air-to-air refuelling scenario, it is also planned to reuse and extend it for formation flight investigations (aiming at saving fuel by surfing the wake of the leader aircraft).



5 ACKNOWLEDGMENTS

The authors would like to thank and acknowledge all colleagues working in the LUBETA project. Sven Geisbauer and Patrick Löchert (both from the DLR Institute of Aerodynamics and Flow Technology) have been tackling the RANS CFD aspects supporting the high-fidelity modelling of the involved aerodynamics effects. Torsten Gerlach, Jan Hettwer, Umut Durak, Jürgen Gotschlich, Sven Oppermann (now at Hochschule Bremen), and Dominik Niedermeier have contributed to the porting of the FMTA model to the AVES simulator, to the implementation of the new features for AAR, and do contribute to all the daily maintenance of the AVES simulation centre. Finally, significant contributions to the virtual cockpit for the receiver as well as to the race-track controller for the tanker were made by Sabrina Stracke as part of her internship and bachelor thesis.

REFERENCES

1. Smith, R. K., 75 years of inflight refueling - Highlights 1923-1998, Air Force History and Museums Program, 1998, ISBN 13: 9780160497797.
2. Jann, T., "Coupled simulation of cargo airdrop from a generic military transport aircraft." Proc. of the 21st AIAA Aerodynamic Decelerator System Technology Conference, Dublin, Ireland, 23–26 May 2011, AIAA 2011-2566.
3. Geisbauer, S., Schade, N., Enk, S., Schmidt, H., and Arnold, J., "Experimental and Numerical Investigation of the Flow Topology During Airdrop Operations," Proc. of the 21st AIAA Aerodynamic Decelerator Systems Technology Conference and Seminar, Dublin, Ireland, 23–26 May 2015, AIAA 2011-2565.
4. Geisbauer, S. and Schmidt, H., "Development and Validation of a RANS-based Airdrop Simulation Approach," Proc. of the 33rd AIAA Applied Aerodynamics Conference, Dallas, TX, USA, 22–26 June 2015, AIAA 2015-3016.
5. Schmidt, H., "Implementierung eines MKS-Fahrwerksmodells in Matlab/Simulink mittels „Response Surfaces“," Tech. rep., DLR (German Aerospace Center) - Institute of Aeroelastics, 2012, IB 232-2013 C 03.
6. Geisbauer, S., "Untersuchung des Einflusses generischer Vorderkantenbeschädigungen auf die aerodynamische Leistungsfähigkeit von Flugzeugprofilen," Tech. rep., DLR (German Aerospace Center) - Institute of Aerodynamics and Flow Technology, 2012, IB 124-2012/903.
7. (NSA), N. S. A., "NATO Standard ATP-3.3.4.2 Air-to-Air Refueling (ATP56), Edition C., Version 1." Tech. rep., NATO, November 2013.
8. Kaden, A. and Luckner, R., "Modeling Wake Vortex Roll-Up and Vortex-Induced Forces and Moments for Tight Formation Flight," Proc. of the 2013 AIAA Modeling and Simulation Technologies Conference, Boston, MA, USA, 19-22 August 2013, pp. 1–16, AIAA 2013-5076.
9. Galle, M., Gerhold, T. and Evans, J., "Technical Documentation of the DLR TAU-Code," Technical Report, DLR-IB 233-97/A43, 1997.
10. Gerhold, T., Galle, M., Friedrich, O., and Evans, J., "Calculation of Complex Three-Dimensional Configurations Employing the DLR-Tau Code," Proc. of the 35th AIAA Aerospace Sciences Meeting and Exhibit, Reno, NV, USA, 1997, AIAA 97-0167.
11. Gerhold, T., Overview of the Hybrid RANS Code TAU, Springer Berlin Heidelberg, Berlin, Heidelberg, 2005, pp. 81–92.
12. Schwamborn, D., Gerhold, T., and Heinrich, R., "The DLR TAU-Code: Recent Applications in Research and Industry," Proc. of the 2006 European Conference on Computational Fluid Dynamics (ECCOMAS CFD), edited by P. Wesseling, E. Oñate, and J. Périaux, TU Delft, Delft, The Netherlands, 2006.
13. Dogan, A. and Blake, W., "Modeling of Bow Wave Effect in Aerial Refueling," Proc. of the 2010 AIAA Atmospheric Flight Mechanics Conference, Toronto, ON, Canada, 2-5 August 2010, pp. 1–17, AIAA 2010-7926.
14. Dogan, A., Blake, W., and Haag, C., "Bow Wave Effect in Aerial Refueling: Computational Analysis and Modeling," Journal of Aircraft, Vol. 50, No. 6, November–December 2013, pp. 1856–1868.
15. Ro, K., Basaran, E., and Kamman, J. W., "Aerodynamic Characteristics of Paratroop Assembly in an Aerial Refueling System," Journal of Aircraft, Vol. 44, No. 3, May-June 2007, pp. 963–970.



16. Haag, C., Schwaab, M., and Blake, W., "Computational Analysis of the Bow-Wave Effect in Air-to-Air Refueling," Proc. of the 2010 AIAA Atmospheric Flight Mechanics Conference, Toronto, ON, Canada, 2-5 August 2010, pp. 1–11, AIAA 2010-7925.
17. Khan, O. and Masud, J., "Trajectory Analysis of Basket Engagement during Aerial Refueling," Proc. of the AIAA SciTech 2014 - Atmospheric Flight Mechanics Conference, National Harbor, MD, USA, 13-17 January 2014, pp. 1–15, AIAA 2014-0190.
18. Bhandari, U., Thomas, P. R., Bullock, S., Richardson, T. S., and du Bois, J. L., "Bow Wave Effect in Probe and Drogue Aerial Refuelling," Proc. of the 2013 AIAA Guidance, Navigation and Control Conference, Boston, MA, USA, 19-22 August 2013, pp. 1–21, AIAA 2013-4695.
19. Spalart, P. and Allmaras, S., "A One-Equation Turbulence Model for Aerodynamic-Flows," La Recherche Aéronautique Journal, No. 1, pp.5-21, 1994.
20. Luckner, R., "Modeling and Simulation of Wake Vortex Encounters: State-of-the-Art and Challenges," Proceedings of the AIAA Modeling and Simulation Technologies Conference, Minneapolis, MN, USA, aug 2012, AIAA-2012-4633.
21. Fischenberg, D., "A Method to Validate Wake Vortex Encounters Models From Flight Test Data," Proceedings of the 27th International Congress of the Aeronautical Sciences, Nice, France, September 2010.
22. Schwarz, C. W., Hahn, K.-U., and Fischenberg, D., "Wake Encounter Severity Assessment Based on Validated Aerodynamic Interaction Models," Proceedings of the AIAA Atmospheric and Space Environments Conference, Toronto, ON, Canada, August 2010, AIAA-2010-7679.
23. Ro, K. and Kamman, J. W., "Modeling and Simulation of Hose-Paradrogue Aerial Refueling Systems," Journal of Guidance, Control and Dynamics, Vol. 33, No. 1, January–February 2010, pp. 53–63.
24. Ro, K., Ahmad, H., and Kamman, J. W., "Dynamic Modeling and Simulation of Hose-Paradrogue Assembly for Mid-Air Operations," Proc. of the 2009 AIAA IntoechAerospace Conference, Seattle, WA, USA, 6-9 April 2009, AIAA 2009-1849.
25. Styuart, A. V., Yamashiro, H., Stirling, R., Mor, M., and Gaston, R., "Numerical Simulation of Hose Whip Phenomenon in Aerial Refueling," Proc. of the 2011 AIAA Atmospheric Flight Mechanics Conference, Portland, OR, USA, 8-11 August 2011, pp. 1–10, AIAA 2011-6211.
26. Vassberg, J. C., Yeh, D. T., Blair, A. J., and Evert, J. M., "Numerical Simulations of KC-10 Centerline Aerial Refueling Hose-Drogue Dynamics With A Reel Take-Up System," Proc. of the 2004 AIAA Applied Aerodynamics Conference and Exhibit, Providence, RI, USA, 16-19 August 2004, pp. 1–19, AIAA 2004-4719.
27. Leitner, R. M. and Estrugo, R., "Numeric Simulation of Aerial Refueling Coupling Dynamics in Case of Hose Reel Malfunction," Proc. of the 2011 AIAA Modeling and Simulation Technologies Conference, Boston, MA, USA, 19-22 August 2011, pp. 1–5, AIAA 2013-4840.
28. Hansen, J. L., Murray, J. E., and Campos, N. V., "The NASA Dryden AAR Project: A Flight Test Approach to an Aerial Refueling System," Proc. of the 2004 AIAA Atmospheric Flight Mechanics Conference and Exhibit, Providence, RI, USA, 16-19 August 2004, AIAA 2004-4939.
29. Zhu, Z. and S.A., M., "Modeling and simulation of aerial refueling by finite element method," International Journal of Solids and Structures, Vol. 44, 2007, pp. 8057–8073, doi:10.1016/j.ijsolstr.2007.05.026.
30. Ro, K., Kuk, T., and Kamman, J. W., "Dynamics and Control of Hose-Drogue Refueling Systems During Coupling," Journal of Guidance, Control, and Dynamics, Vol. 34, No. 6, November–December 2011, pp. 1694–1708, DOI: 10.2514/1.53205.
31. Dibley, R. P., Allen, M. J., and Nabaa, N., "Autonomous Airborne Refueling Demonstration Phase I Flight-Test Results," Proc. of the 2007 AIAA Atmospheric Flight Mechanics Conference and Exhibit, Hilton Head, SC, USA, 20-23 August 2007, pp. 1–19, AIAA 2007-6639.
32. Dibley, R. P., Allen, M. J., and Nabaa, N., "Autonomous Airborne Refueling Demonstration Phase I Flight-Test Results," Tech. rep., Dryden Flight Research Center, Edwards, CA, USA, 2007, NASA/TM-2007-214632.
33. Duda, H., Gerlach, T., Advani, S., and Potter, M., "Design of the DLR AVES Research Flight Simulator," Proc. of the 2013 AIAA Modeling and Simulation Technologies Conference, Boston, MA, USA, 19-22 August 2013, pp. 1–14, AIAA 2013-4737, DOI: 10.2514/6.2013-4737.
34. Gerlach, T. and Durak, U., "AVES SDK: Bridging the Gap between Simulator and Flight Systems Designer," Proc. of the AIAA AVIATION 2015 Modeling and Simulation Technologies Conference, Dallas, TX, USA, 22-26 June 2015, pp. 1–10, AIAA 2015-2947.



35. Gerlach, T., Durak, U., Knüppel, A., and Rambau, T., "Running High Level Architecture in Real-Time for Flight Simulator Integration," Proc. of the AIAA AVIATION 2016 Modeling and Simulation Technologies Conference, Washington, D.C., USA, 13-17 June 2016, pp. 1–10, AIAA 2016-4130.
36. Burns, R. S. and Clark, C. S., "The Automated Aerial Refueling Simulation at the AVTAS Laboratory," Proc. of the 2005 AIAA Modeling and Simulation Technologies Conference and Exhibit, San Francisco, CA, USA, 15-18 August 2005, AIAA 2005-6008.
37. Williams, R. D., Feitshans, G. L., and Rowe, A. J., "A Prototype UAV Control Station Interface for Automated Aerial Refueling," Proc. of the 2005 AIAA Modeling and Simulation Technologies Conference and Exhibit, San Francisco, CA, USA, 15-18 August 2005, AIAA 2005-6009.
38. Gerlach, T., "Visualisation of the brownout phenomenon, integration and test on a helicopter flight simulator," RAeS The Aeronautical Journal, Vol. 114, No. 1163, January 2011, pp. 57–63, DOI: <https://doi.org/10.1017/S0001924000005364>.
39. Gunetti, P., Cassaro, M., Battipede, M., and Gili, P., "Modeling Autopilot Suites For A Multi-Aircraft Simulator," Proc. of the 2013 AIAA Modeling and Simulation Technologies Conference, Boston, MA, USA, 19-22 August 2013, pp. 1–15, AIAA 2013-4736.
40. Fezans, N. and Jann, T., "Modeling and Simulation for the Automation of Aerial Refueling of Military Transport Aircraft with the Probe-and-Drogue System," Proc. of the AIAA Modeling and Simulation Technologies Conference, AIAA AVIATION 2017, Denver, CO, USA, June 2017, AIAA-2017-4008, DOI: <https://arc.aiaa.org/doi/abs/10.2514/6.2017-4008>.
41. Stracke, S., "Development of a Tanker Trajectory Tracking Flight Control Function During Aerial Refuelling," (original German title: "Entwicklung eines Flugreglers zur Einhaltung der Flugbahn des Tankers bei der Luftbetankung"), Bachelor Thesis, FH Aachen University of Applied Sciences, 2016. DLR-IB-FT-FS-2016-334.